Volume 1 | Number 1 | Jan 2013 | Pages 1–100

## Journal of
## Materials Chemistry B

Materials for biology and medicine
www.rsc.org/materialsB

ROYAL SOCIETY
OF CHEMISTRY

ROYAL SOCIETY
OF CHEMISTRY

www.rsc.org/materialsB

**ARTICLE TYPE**

# Fabrication of a novel biomaterial with enhanced mechanical and conducting properties

**Pranav C. Khandelwal**[a,b]**, Suchi S. Agrawal**[a]**, Manoj A. G. Namboothiry**[b]**,Namrata Gundiah\***[a]

Conducting polymers combine the advantages of metal conductivity with ease in processing and biocompatibility; making them extremely versatile for biosensor and tissue engineering applications. However, the inherent brittle property of conducting polymers limits their direct use in such applications which generally warrant soft and flexible material responses. Addition of fillers increases the material

10 compliance, but is achieved at the cost of reduced electrical conductivity. To retain suitable conductivity without compromising the mechanical properties, we fabricate an electroactive blend (dPEDOT) using low grade PEDOT:PSS as the base conducting polymer with polyvinyl alcohol and glycerol as dopants. Bulk dPEDOT films show a thermally stable response till 110 ℃ with over seven fold increase in room temperature conductivity as compared to 0.002 Scm$^{-1}$ for pristine PEDOT:PSS. We characterized the

15 nonlinear stress-strain response of dPEDOT, well described using a Mooney-Rivlin hyperelastic model, with ductility of ~five times its original length and report elastomer-like moduli. Dynamic mechanical analysis shows constant storage moduli over a large range of frequencies with corresponding linear increase in tan (δ) values. We relate the enhanced performance of dPEDOT with the underlying structural constituents using FTIR and AFM microscopy. These data demonstrate specific interactions between

20 individual components of dPEDOT, their effect on surface topography and material properties. Finally, we show biocompatibility of dPEDOT using fibroblasts that have comparable cell morphologies and viability as control; making it attractive as a biomaterial.

## Introduction

Electroactive polymeric scaffolds have the potential to
25 revolutionize tissue engineering, drug delivery, biosensor and actuator applications through tailoring of properties to impart desirable electrical, electrochemical and electromechanical stimuli[1]. Optimizing the mechanical and electrical properties of polymer blends is a key requirement for these applications whilst
30 providing essential physio-chemical and biological cues for cell adhesion/proliferation and migration. Among conducting polymers, poly(3,4-ethylenedioxythiophene), PEDOT, with a balancing counter-ion, sodium polystryrenesulphonate, PSS, as dopant is a promising biocompatible material with good thermal,
35 electrical and chemical stability[2–5]. However, a key disadvantage in using PEDOT:PSS for biological applications is its inherent high Young's modulus and low ductility[6]. Blending of polyvinyl alcohol (PVA), a water soluble polymer, to PEDOT:PSS enhances the ductility and flexibility but lowers the overall
40 conductivity of the network[7,8]. The goals of this study are to fabricate an electroactive and stretchable material for tissue engineering applications using PEDOT:PSS as a model system. We incorporate biocompatible dopants, such as glycerol and PVA, to create a composite blend that emulates the physiological
45 mechanical conditions while enhancing the electrical characteristics of the polymer.

## Materials and Methods

### Synthesis and fabrication of composite PEDOT:PSS films

Base conducting PEDOT:PSS (CLEVIOS™ P VP AI 4083,
50 Heraeus, Germany), glycerol ($M_w$ = 92.10 gmol$^{-1}$) and PVA ($M_w$ = 85,000-1,24,000 gmol$^{-1}$) were mixed in weight ratios of 80:12.5:7.5 and stirred for 3 hours at 80 ± 5 ℃ to form a homogeneous blend (dPEDOT) that was used in the study.

### Mechanical characterization of bulk dPEDOT films

55 ASTM D882 standard was used to prepare rectangular specimens for mechanical experiments by air drying the blend in a mould for 12 hours. Monotonic tension experiments were performed using a mechanical testing system (Bangalore Integrated System Solutions (P) Ltd, India), details of which are elsewhere[9].
60 PVA/glycerol and pristine hydrated PEDOT:PSS films, prepared *via* drop casting followed by drying at 40 ℃ for 12 hours, were used as controls in the study. Specimens were clamped to the stretcher arms and tested to failure under displacement control (0.02 mms$^{-1}$). Engineering stress-strain data, obtained on
65 PVA/glycerol and dPEDOT specimens, were fit to a neo-Hookean (NH) form of hyperelastic constitutive model, given by $\psi_{NH} = c_o(\lambda_1^2 + \lambda_2^2 + \lambda_3^2 - 3)$ where $\lambda_i; i = 1:3$ are stretches in the principal directions respectively. These experimental data

were also fit to a Mooney-Rivlin (MR) form given by $\psi_{MR} = c_1(\lambda_1^2 + \lambda_2^2 + \lambda_3^2 - 3) + c_2(\lambda_1^{-2} + \lambda_2^{-2} + \lambda_3^{-2} - 3)$. Unknown coefficients to the models ($c_0, c_1$ and $c_2$) were obtained using a nonlinear least squares minimization routine employing the

5  *lsqnonlin* function in MATLAB (v7.8.0.347 R2009a) and were reported corresponding to the maximum coefficient of determination ($r^2$) obtained using 25 different initial guesses. To quantify viscoelastic properties of the fabricated blend, films were clamped to a Bose Electroforce® 3200 testing system (Bose

10  Corp., USA) and stretched using cyclic (0.01-100 Hz) sinusoidal strains ranging from 0 to 5%. A custom written routine was employed to analyse the load and displacement traces to compute the storage ($E'$) and loss moduli ($E''$). The corresponding phase angle ($\delta$) was next obtained as based on the ratio of $E''$ to $E'$.

15  **Conductivity of dPEDOT films**

A four probe van der Pauw method was used to measure the conductivity of the fabricated thin films. Square 18 mm cover slips, pre-treated in piranha solution (3:1; $H_2SO_4$:6wt%$H_2O_2$), were spin coated with dPEDOT at 2000 rpm for 60 seconds and

20  cured at 100 ˚C for 20 minutes in an oven. A DC probe station (Agilent Device Analyzer B1500A, USA) recorded the sheet resistance ($R_s$), using silver ohmic contacts at four corners of the dPEDOT film, by heating from 30 to 160 ˚C in steps of 10 ˚C. $R_s$ was calculated by averaging the eight permutations in resistance

25  measurements ($R_{avg}$), obtained between two individual silver contacts at each time, and given by $R_s = \pi (R_{avg}/\ln2)$. Based on experimentally determined $R_s$ values, conductivity ($\kappa$) was calculated as $\kappa = 1/(R_s t)$. The film thickness (t) was independently determined using a 3D non-contact optical profilometer (CCI MP

30  3D, Taylor Hobson, UK) for each batch of samples prepared under identical conditions.

**FTIR spectroscopy**

Specimens of PVA, PVA/glycerol, PEDOT:PSS and dPEDOT were drop cast onto p-type silicon wafers of 1-10 Ω cm resistivity

35  and dried in an oven at 40 ˚C for 12 hours to obtain thin films. A single beam Fourier transform infrared spectrophotometer (Thermo Fisher Scientific, USA) was used in transmittance mode with (7-10) x$10^{-3}$ W laser power to record vibrations in 4000 to 400 cm$^{-1}$ range with a scanning resolution of 4 cm$^{-1}$.

40  **Characterization of surface topography using Atomic Force Microscopy (AFM)**

Spin coated control (PVA/glycerol) and dPEDOT specimens were prepared as described earlier and scanned using a PARK NX 10 (Park systems, Korea) AFM in tapping mode. A 40 Nm$^{-1}$

45  stiffness cantilever, with scanning rate of 0.8 Hz and a resolution of 256 scan lines, was used to produce height and phase images. Five locations on each individual sample were scanned to obtain images with windows of 5 µm x 5 µm and 0.5 µm x 0.5 µm respectively. The images were processed using custom XEI

50  (4.1.0) software provided by the manufacturer.

**Biocompatibility of dPEDOT**

Spin coated dPEDOT cover slips were dessicated overnight, placed in tissue culture plates and sterilized using graded ethanol solutions (30%, 50% and 70%) for 10 minutes. Specimens were

55  next washed thrice with phosphate buffered saline and coated

with fibronectin (FN, Sigma Aldrich F2006; 50 µgml$^{-1}$). To test biocompatibility of dPEDOT, films were cultured with ~2x$10^5$ cells/ml NIH/3T3 fibroblasts and analysed for changes in morphology and viability using FN-coated cover slips as positive

60  control. To observe the cell morphology, specimens were fixed with 4% formaldehyde, permeabilized with 0.5% Triton X-100 and stained using rhodamine-conjugated phalloidin (Molecular Probes) to visualize actin networks, labelled in red, and DAPI which stains the nucleus blue. Specimens were imaged using a

65  Leica DMI-6000B confocal microscope (63X objective) with FN coated coverslips as control. Cell viability was assessed using FN-coated dPEDOT and control coverslips which were seeded with cells for 24 hours and treated with 1X trypsin-EDTA solution to allow for cell detachment. Trypsin was next

70  deactivated with DMEM medium supplemented with 10% FBS and the individual cells were collected by centrifugation. Cells were washed and resuspended in 200 µL PBS. Flow cytometry (BD FACSVerse, Becton Dickinson, USA) was used to analyse the fraction of live/ dead cells using propidium iodide (PI, 1

75  mg/mL) that stains the nuclei of dead cells. A 586±21 nm laser was used to detect cells positive for the PI dye. Three sets of data were acquired, each set corresponding to 10,000 cells, which were analysed using FACSDiva 6.1.3 software.

**Statistics**

80  Data are presented as the mean ± standard deviation. Significant differences, if any, between control and dPEDOT specimens were assessed using the Student's *t*-test where p≤0.05 was considered statistically significant.

85  **Results and Discussion**

Stretchable conducting and biocompatible polymers hold promise over a spectrum of applications including sensing, soft robotics, and biomedical applications. Current literature on conducting polymers shows that an increase in conductivity may be achieved

90  through use of suitable dopants. However, few studies have focussed on concomitantly increasing the conductivity without compromising the stretchability of polymers films. In this study, we enhance the conductivity of PEDOT:PSS films using glycerol as a dopant and achieve rubber-like mechanical characteristics of

95  the doped blend using PVA. The fabricated dPEDOT is extensible to several times its original length and has significantly higher conductivity as compared to pristine PEDOT:PSS. There are five implications of our work; first, strain to failure of dPEDOT is higher by about six fold as compared to a more

100  brittle-like response of PEDOT:PSS. Further, we achieve elastomer-like moduli for dPEDOT blend as compared to pristine PEDOT:PSS. Second, the increase in conductivity of bulk dPEDOT is over seven fold which may primarily be due to presence of glycerol in the blend. Third, we show that

105  interactions between individual dopants with base material in dPEDOT aid in enhancing conductivity and also affect the surface morphology of doped blend. Fourth, reaction between glycerol and PEDOT:PSS imparts water resistant characteristics to the blend which may be essential for many sensing

110  applications. Fifth, results from flow cytometry and confocal

imaging indicate unaltered cell viability and morphology on dPEDOT as compared to controls.
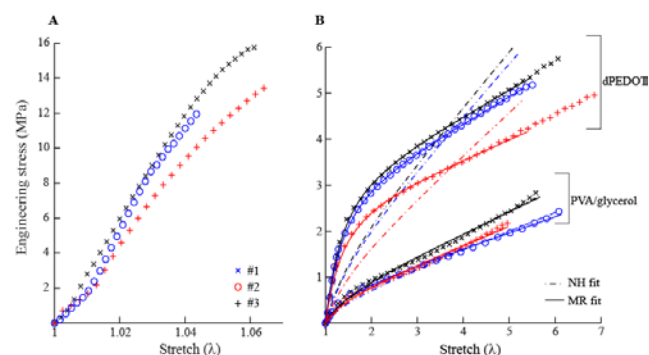


**Figure 1A.** Uniaxial mechanical tests were used to obtain stress-strain
5 data from base PEDOT:PSS(1:6) films stretched to failure under displacement control. **B**. In contrast, dPEDOT and PVA/glycerol films undergo large deformation. Data fits from NH and MR forms of strain energy function to dPEDOT specimens are shown.
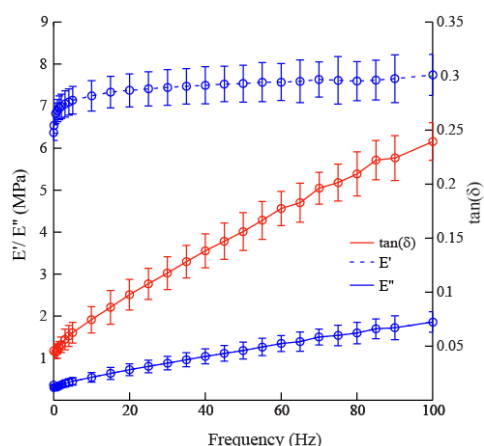


10 **Figure 2**. Data from DMA experiments performed on the dPEDOT samples (n=3) are plotted to show variations in the storage ($E'$) and loss ($E''$) moduli with frequency. Also shown on the same plot are results from tan($\delta$), calculated as a ratio of loss to storage moduli.

**Comparative differences in the mechanical properties of**
15 **dPEDOT films with control**

Pristine PEDOT:PSS films (n=3), stretched uniaxially to failure, had a stiff and relatively linear mechanical response (Figure 1A). Material modulus was calculated to be 0.31±0.04 GPa with a stretch at failure of 5.79±1.14. Our data are however lower than
20 those reported for PEDOT:PSS cast films (1.8±0.2GPa) that were of a superior grade (1:2) as compared to the1:6 grade used in this study[10]. In contrast, control (PVA/glycerol) films (n=3) showed a highly nonlinear stress-strain response with moduli of 1.66±0.16 MPa and did not fail even when stretched to ~six times their
25 initial length (Figure 1B). dPEDOT films (n=3) also exhibit a similar stress-strain response with measured moduli of 6.31±0.89 MPa.
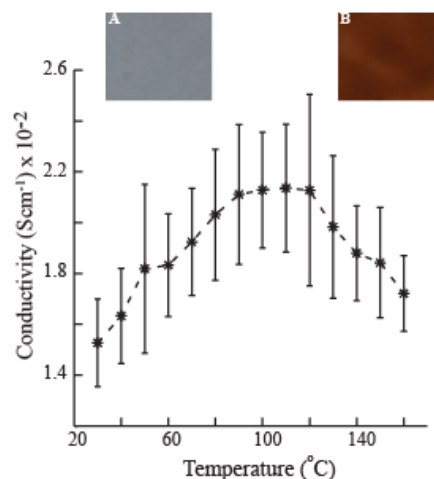


**Figure 3.** Thermal conductivity of dPEDOT samples was measured over a
30 broad temperature range. Insets A and B show images of samples obtained before and after thermal conductivity measurements to illustrate changes in the sample due to heating.

Hence, these films show a composite behavior that is characteristic of the individual components comprising the blend
35 with a stiffness higher than PVA/glycerol and lower than that of PEDOT:PSS. To model the material response, stress-strain data from dPEDOT samples were fit to NH and MR strain energy functions. A stretch range from 1 to 5 was selected to obtain the unknown coefficients in the two models (Figure 1B). The NH
40 model is equivalent to a statistical mechanical treatment corresponding to a Gaussian distribution of long chain polymers. However, the MR model captures the stiffening response at higher deformations in rubber-like materials[9]. MR model had $r^2$>0.998 for each of the dPEDOT samples in the study with
45 coefficients $c_1$ (0.25±0.04 MPa) and $c_2$ (1.05±0.11 MPa) similar to that reported for elastomers[11]. In contrast, the NH model had low $r^2$ fits (0.648-0.728) with coefficient $c_0$ of 0.53±0.06 MPa. Our data for dPEDOT blends are better captured using the MR model rather than the NH model. These results suggest that
50 mechanisms either related to chain stiffening at larger extensions or the presence of stiffer functional groups in the blend may both be responsible for these observed effects.

Figure 2 shows the average (± std) values of dynamic stress-strain properties for $E'$, $E''$ and tan($\delta$) on bulk dPEDOT samples
55 (n=3). $E'$ values plateau over a range of frequencies from 35-100 Hz whereas $E''$ shows a steady increase over the tested range of frequencies which indicate increasing viscous losses in the material at higher frequencies. Further, tan($\delta$) also increases steadily from 0.01 to 100 Hz without any apparent phase
60 transitions measured at room temperature. These results suggest an overall mechanical behaviour for the blend which has elastomer-like material properties, including high strain to failure as compared to base PEDOT:PSS, and is stable over a wide range of frequencies.

65 **Thermal conductivity map of dPEDOT films**

Figure 3 shows conductivity measurements obtained on dPEDOT films using the four probe method as described earlier. Specimens have a stable response in κ with values of 0.015±0.002 Scm$^{-1}$ at 30 ˚C and a peak value of 0.021±0.002 Scm$^{-1}$ at 110 ˚C[12].

However, following the gradual increase until 110 ˚C, we observe a decrease in κ which may be related to sample degradation visualized as a change in color (insets 3A and 3B).
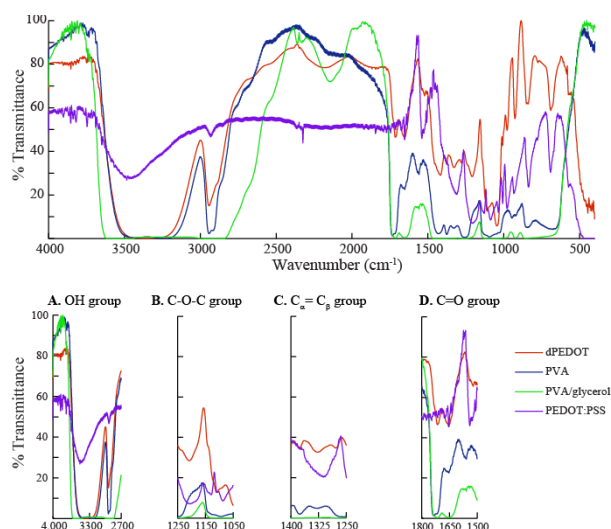


**Figure 4.** FTIR spectra are shown for PVA, PVA/glycerol, PEDOT:PSS and dPEDOT specimens in transmission mode. **A**. Broad peak corresponding to O-H vibrations in PVA/glycerol compared to that in dPEDOT is visible. **B**. Characteristic C-O-C peaks of PEDOT with corresponding shifts in dPEDOT are clearly seen. **C**. Characteristic peak of $C_\alpha=C_\beta$ vibrations in dPEDOT that is indicative of the quinoid ring structure in a well doped PEDOT is observed. **D**. Shift in peak of C=O of PVA in dPEDOT at 1714 cm$^{-1}$ is indicative of interaction of PVA in doped material.

We hypothesize that the 7.63±0.86 fold increase in κ of dPEDOT in contrast to base PEDOT:PSS[13] may be due to presence of the dopant, glycerol. Presence of glycerol promotes swelling and aggregation of PEDOT rich particles and permits esterification of the sulphonic ($SO_3^-$) groups in PSS; imparting water resistant characteristics to dPEDOT[14,15]. In contrast, PVA, with a base conductivity[16] of $1.4 \times 10^{-9}$ Scm$^{-1}$, acts as insulating filler[17] and reduces the overall negative charge of $SO_3^-$ groups of PSS through hydrogen bonding. This decreases the ability of sulphonic groups to act as a counter ion in the PEDOT:PSS moiety[17]. Further, increase in the concentration of PVA, acting as filler, may reduce the availability of free conducting paths[8]. Thus, addition of glycerol to the blend is essential to compensate the conductivity drop due to PVA[18].

### Characterization of chemical interactions in dPEDOT

FTIR spectra of dPEDOT films were obtained to investigate the presence and interactions amongst the various constituents in the doped material (Figure 4). Characteristic spectra demonstrating their contributions to the observed properties are highlighted in the subplots. Specific functional groups identifying the presence of PEDOT:PSS in the blend are indicated through presence of C-S bonds in the thiophene ring of PEDOT, seen at 690, 838 and 977 cm$^{-1}$ and vibrations of $SO_3^-$ group of PSS, seen at 1043 cm$^{-1}$ in dPEDOT[19,20]. Peaks appearing in PEDOT:PSS at 1205, 1128 and 1088 cm$^{-1}$ which represent C-O-C ring stretching of the ethylene dioxy group[19] do not however appear at similar wavenumbers in dPEDOT (Figure 4B). This suggests interaction

of base PEDOT:PSS with the underlying constituents. Specifically, the presence of a broader peak of O-H vibrations in PVA/glycerol (3630 to 2820 cm$^{-1}$)[21,22] as compared to that in dPEDOT (3500 to 3200 cm$^{-1}$) (Figure 4A) suggests interactions between the O-H group in PVA with the $SO_3^-$ group of PSS that causes an insulating filler effect in dPEDOT[17]. Additional interactions of PVA with PEDOT:PSS is indicated by a shift in the characteristic peak at 1730 cm$^{-1}$ in pure PVA[21] to 1714 cm$^{-1}$ in dPEDOT (Figure 4D); attributed to the stretching vibration of the C=O bonds in vinyl acetate group of PVA[23].

To explore the reaction of glycerol with base PEDOT:PSS, we identify interactions between C-O-H group of glycerol and PEDOT:PSS through a shift in the peak corresponding to the C-O vibrations of glycerol appearing at 2181 cm$^{-1}$ in dPEDOT as compared to 2143 cm$^{-1}$ in PVA/glycerol[22]. Further, peaks corresponding to the presence of O-H vibrations in glycerol are decreased in dPEDOT as compared to the PVA/glycerol mixture (Figure 4A). These results indicate esterification of $SO_3^-$ by alcohol end groups which impart water resistant properties to dPEDOT[15]. Finally, the appearance of a peak in dPEDOT at 1329 cm$^{-1}$ which corresponds to $C_\alpha=C_\beta$ vibrations[20] of a five membered quinoid resonant structure of PEDOT, is indicative of a well doped material[24] (Figure 4C). These data suggest that addition of glycerol leads to a structural reorientation of PEDOT:PSS chains in dPEDOT which is responsible for the increase in conductivity of the blend[24].

### Distinct structural features of dPEDOT using AFM

To visualize and assess the role of individual constituents of dPEDOT in the surface properties of the doped blend, we used height images of dPEDOT (Figure 5A) and control (PVA/glycerol) films (Figure 5B) obtained from an AFM. Clear differences exist in the surface roughness of control and dPEDOT films (Figure 5). The $R_a$ for dPEDOT was 2.26±0.28 nm as compared to 37.79±9.65 nm of control specimens that shows a smoother surface for dPEDOT specimens. To investigate the reasons for decrease in surface roughness of dPEDOT films, we used phase and height images on a 500 nm x 500 nm region (Figure 6A, B).
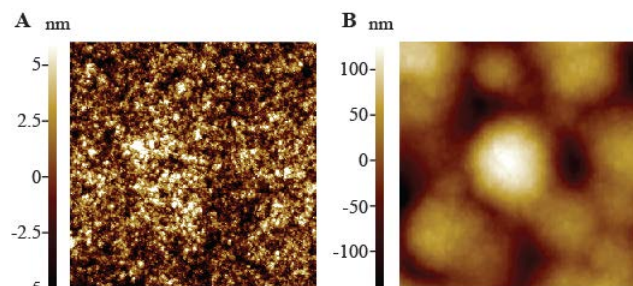


**Figure 5.** AFM was used to characterize the surface topography of dPEDOT and control specimens imaged using a 5 µm x 5 µm area. **A**. dPEDOT specimens show uniform grain-like structure. **B**. In contrast, control samples have large globules with higher roughness as compared to dPEDOT.

Characteristic bright aligned regions are seen in the phase images of dPEDOT with an approximate particle size of 70-80 nm which is in agreement with that given by the manufacturer[13]. Uniform bright regions in the phase image (Figure 6C) suggest aggregation of PEDOT chains, with the core surrounded by dark regions of PSS[25,26], which may be caused due to the addition of glycerol to enhance film conductivity. The
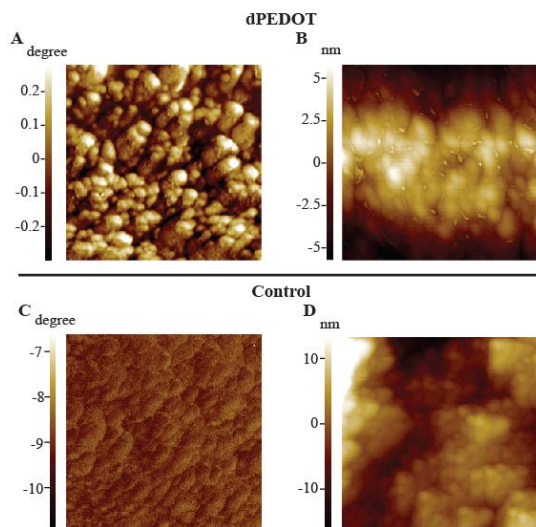


**Figure 6.** Phase and height images of dPEDOT and control specimens were obtained and are shown over a 0.5 µm x 0.5 µm area. **A.** Bright phase regions show presence of coalesced PEDOT rich regions. **B.** Aggregation of grains is seen. **C.** Control samples show negligible phase contrast **D.** High surface roughness with small particle size forming the globule are visible in control samples that correspond to PVA and glycerol.

Figure 6D which shows smaller unaligned units of PVA/glycerol corresponding phase (Figure 6C) and height images (Figure 6D) for control (PVA/glycerol) films are shown as comparison in with particle dimensions smaller than that of PEDOT:PSS. Smaller particle sizes for unaligned units may be responsible for the large variations in surface roughness. Larger polymeric PVA chains, with $M_w$ = 85,000-1,24,000 gmol$^{-1}$, settle down during curing and permit the smaller PEDOT:PSS moiety to the surface; thereby reducing the surface roughness of dPEDOT dramatically.

### Biocompatibility of composite blends

Because the individual components of dPEDOT are used in numerous biological applications[27,28], we used flow cytometry and confocal microscopy to assess the biocompatibility of dPEDOT films using 3T3 fibroblast cells. FN coated cover slips as positive controls (Figure 7A) and FN coated dPEDOT samples (Figure 7B) were cultured with fibroblasts and stained to observe the cell morphology. Autofluorescence of the doped films present some challenges in visualizing fluorescently labelled proteins in the cell. The overall morphology, defined by stretched filamentous actin networks with the DAPI stained nuclei, appears similar on both substrates. Cell viability on FN coated control and FN coated dPEDOT films was quantified using flow cytometry to assess the growth rates of cells following 24 hour culture (Figure 8). These data show the percentage of live cells to be 91.90±5.09 and 95.47±1.20 on FN coated coverslips and

dPEDOT samples respectively (Figure 8A, 8B) which are not statistically different (p=0.303). Histograms comparing cell viability on control and dPEDOT substrates are also shown which indicate significant overlap in the peaks (Figure 8C). Together, these results show that dPEDOT films have suitable surface characteristics for FN adsorption to aid cell adhesion and proliferation. Additional studies are warranted to quantify the effects of electric field on fibroblasts and on the long term viability of cells on the novel dPEDOT substrate.
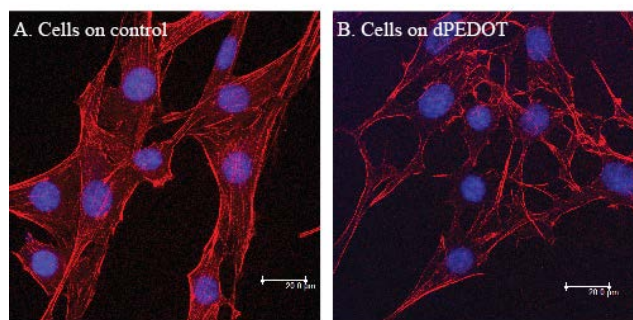


**Figure 7A.** Image of 3T3 fibroblasts cultured on FN coated control coverslips and stained for actin and nuclei are shown for control. **B.** Cells were also seeded on spin coated coverslips of dPEDOT and show similar morphologies. Scale bar is 20 µm.
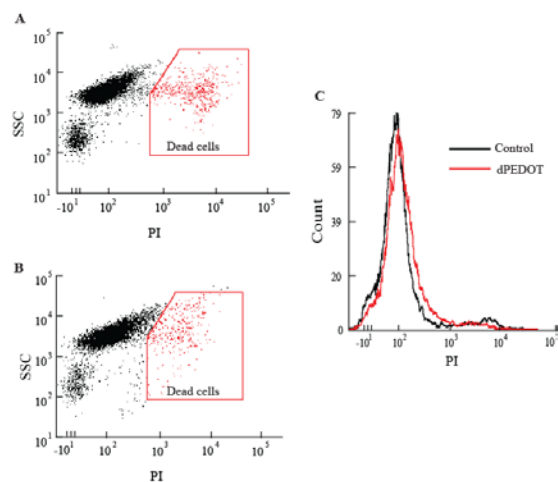


**Figure 8.**Results from flow cytometry studies to assess cell viability are shown. A 2D dot plot displaying the intensity of propidium iodide with side scatter indicative of cellular complexity (SSC) on control (**A**) and dPEDOT (**B**) are shown which are indicative of the extent of cell death. The histogram data from dPEDOT and control specimens are not significantly different. (**C.**)

### Conclusions

In this study, we fabricated a novel electroactive polymer blend using PEDOT:PSS with glycerol as a dopant and PVA as a filler material. Presence of PVA in the blend makes the blend tough and mechanically compliant, albeit has an adverse effect on the conductivity of the base polymer PEDOT:PSS. We report rubber-

like moduli (6.31±0.89 MPa) for dPEDOT blend and high stretch ability of 5.79±1.14 times as compared to a relatively brittle-like response for pristine PEDOT:PSS. These stress-strain responses for dPEDOT are well described using a MR fit over the entire range of deformations. DMA experiments reveal no phase transitions when tested at room temperature with almost constant $E'$ over a large range of frequencies; indicating a relatively stable mechanical response. To increase the conductivity of base PEDOT:PSS, we use glycerol as a dopant that compensates for the conductivity loss of the low grade PEDOT:PSS to produce a 7.63±0.86 fold conductivity increase to 0.015±0.002 Scm$^{-1}$. FTIR analysis confirm interactions of the constituents in dPEDOT and their individual contributions to both enhancing the conductivity of PEDOT:PSS and the appearance of water resistant properties to the doped blend. Further, AFM studies show islands of aligned PEDOT with a surrounding mantle of PSS that have a smooth morphology as compared to rougher PVA/ glycerol mixtures.To establish the viability of dPEDOT as tissue engineered scaffolds, we also confirm cell viability and biocompatibility using flow cytometry assay and confocal microscopy. Together, these properties make dPEDOT an attractive material that can be used in soft robotics, tissue engineering and biosensing applications which demand robust and stable thermo- mechanical performance.

## Acknowledgements

## Notes and references

$^a$ *Department of Mechanical Engineering, Indian Institute of Science, Bangalore - 560012, Karnataka, India. Tel: +91 80 2293 2860; E-mail: namrata@mecheng.iisc.ernet.in; ngundiah@gmail.com*

$^b$ *School of Physics, Indian Institute of Science Education and Research, Computer Science Building, College of Engineering Trivandrum Campus, Thiruvananthapuram - 695016,Kerala, India.*

† No conflicts of interest

1. R. Balint, N. J. Cassidy, and S. H. Cartmell, *Acta Biomater.*, 2014, **10**, 2341-2353.
2. S.-C. Luo, E. Mohamed Ali, N. C. Tansil, H.-H. Yu, S. Gao, E. A. B. Kantchev, and J. Y. Ying, *Langmuir*, 2008, **24**, 8071–7.
3. V. Karagkiozaki, P. G. Karagiannidis, M. Gioti, P. Kavatzikidou, D. Georgiou, E. Georgaraki, and S. Logothetidis, *Biochim. Biophys. Acta*, 2013, **1830**, 4294–304.
4. J. E. Collazos-Castro, J. L. Polo, G. R. Hernández-Labrado, V. Padial-Cañete, and C. García-Rama, *Biomaterials*, 2010, **31**, 9244–55.
5. S. Kirchmeyer and K. Reuter, *J. Mater. Chem.*, 2005, **15**, 2077.
6. U. Lang, N. Naujoks, and J. Dual, *Synth. Met.*, 2009, **159**, 473–479.
7. C. Chen, A. Torrents, L. Kulinsky, R. D. Nelson, M. J. Madou, L. Valdevit, and J. C. LaRue, *Synth. Met.*, 2011, **161**, 2259–2267.
8. C. Chen, J. C. LaRue, R. D. Nelson, L. Kulinsky, and M. J. Madou, *J. Appl. Polym. Sci.*, 2012, **125**, 3134–3141.
9. A. R. Babu and N. Gundiah, *Exp. Mech.*, 2014, **54**,1177-1187.
10. H. Okuzaki and M. Ishihara, *Macromol. Rapid Commun.*, 2003, **24**, 261–264.
11. A. Vieyres, R. Pérez-Aparicio, P.-A. Albouy, O. Sanseau, K. Saalwächter, D. R. Long, and P. Sotta, *Macromolecules*, 2013, **46**, 889–899.
12. P.K. Khandelwal, Masters thesis in Physics, Indian Institute of Science Education and Research, Thiruvananthapuram, April, 2014.
13. C. P. D. Heraeus, *Clevios $^{TM}$ p vp ai 4083*, 2010.
14. S. Ghosh and O. Inganäs, *Synth. Met.*, 2001, **121**, 1321–1322.
15. A. B. Rodríguez, M. M. Voigt, S. J. Martin, T. J. Whittle, R. M. Dalgliesh, R. L. Thompson, D. G. Lidzey, and M. Geoghegan, *J. Mater. Chem.*, 2011, **21**, 19324.
16. E. Sheha, M. Nasr, and M. K. El-Mansy, *Phys. Scr.*, 2013, **88**, 035701.
17. N. Romyen, S. Thongyai, P. Praserthdam, and G. A. Sotzing, *J. Mater. Sci. Mater. Electron.*, 2013, **24**, 2897–2905.
18. J. Suarez-Vargas, M. Calderon, W. Bramer-Escamilla, S. Briceno, I. Sanchez, P. Bolano, C. Caputo, *Rev. LatinAm. Metal. Mat.*, 2014, **35**.
19. X. Zhang, D. Chang, J. Liu, and Y. Luo, *J. Mater. Chem.*, 2010, **20**, 5080.
20. J. W. Choi, M. G. Han, S. Y. Kim, S. G. Oh, and S. S. Im, *Synth. Met.*, 2004, **141**, 293–299.
21. M. F. H. Attia, G.; Abd El-kader, *Int. J. Electrochem. Sci.*, 2013, **8**, 5672–5687.
22. A. M. M. . Hidawati, E. N.; Sakinah, *Int. J. Chem. Environ. Eng.*, 2011, **2**, 309–313.
23. F. Ahmad and E. Sheha, *J. Adv. Res.*, 2013, **4**, 155–161.
24. J. Ouyang, Q. Xu, C.-W. Chu, Y. Yang, G. Li, and J. Shinar, *Polymer (Guildf).*, 2004, **45**, 8443–8450.
25. U. Lang, E. Müller, N. Naujoks, and J. Dual, *Adv. Funct. Mater.*, 2009, **19**, 1215–1220.
26. A. M. Nardes, M. Kemerink, R. A. J. Janssen, J. A. M. Bastiaansen, N. M. M. Kiggen, B. M. W. Langeveld, A. J. J. M. van Breemen, and M. M. de Kok, *Adv. Mater.*, 2007, **19**, 1196–1200.
27. X. Yang, K. Yang, S. Wu, X. Chen, F. Yu, J. Li, M. Ma, and Z. Zhu, *Radiat. Phys. Chem.*, 2010, **79**, 606–611.
28. G. Paradossi, F. Cavalieri, E. Chiessi, C. Spagnoli, and M. K. Cowman, *J. Mater. Sci. Mater. Med.*, 2003, **14**, 687–691.